Demonstrating the Potential of Arrayed–Waveguide Grating Based Single–Hop WDM Networks

Martin Maier and Adam Wolisz

Abstract— **Single-hop WDM networks have several desirable features such as high channel utilization, inherent transparency and simplified network management. As opposed to the passive star coupler (PSC), the arrayed-waveguide grating (AWG) is a wavelength routing device which allows spatial wavelength reuse. Given N simultaneously transmitting nodes, $\lceil \sqrt{N} \rceil$ wavelengths are required in an AWG based single-hop network compared to N wavelengths in a PSC based single-hop network. Due to the reduced wavelength pool size in AWG based WDM networks, tunable transmitters with a negligible tuning time can be deployed resulting in a significantly smaller tuning penalty. In this paper it is shown analytically that for fixed channel assignment the AWG clearly outperform the PSC in terms of aggregate throughput, mean queueing delay and packet loss. However, due to the assumption of single-packet buffers the blocking probability grows rapidly with increasing traffic for both PSC and AWG.**

Keywords— **Wavelength division multiplexing (WDM), arrayed-waveguide grating (AWG), passive star coupler (PSC), buffer- and switchless single-hop networks, spatial wavelength reuse, transceiver tuning penalty**

I. Introduction

OPTICAL networks provide some very desirable properties such as huge bandwidth, low fiber loss, low error rates and low costs. Future optical networks will have a slim protocol stack without ATM and SONET/SDH layers resulting in a significantly reduced overhead and network complexity. IP datagrams will be directly transmitted over optical networks using wavelength division multiplexing (WDM). In WDM networks, the optical bandwidth is partitioned into a number of separate channels whose line rate match the transmission speed of electronic devices.

Generally, WDM networks can be classified into single-hop and multihop networks. In multihop networks each packet traverses a number of intermediate nodes until it reaches its destination [1]. At each intermediate node the packet is converted into the electronic domain, processed and finally reconverted into the optical domain and forwarded. Due to the very high optical transmission rates electronic processing devices are very expensive or even unfeasible at present. As a consequence, the huge optical bandwidth cannot exploited entirely resulting in electro-optic bottlenecks.

Several approaches which avoid electro-optic bottlenecks have been proposed. An overview of the various photonic packet switching techniques is given in [2]. Among the most popular switching techniques are optical label switching (OLS), optical burst switching (OBS), optical packet switching (OPS) and photonic slot routing (PSR). All of them have in common that they help realize so-called all-optical networks. In all-optical networks packets remain in the optical domain until they reach the destination nodes. Even though those techniques prevent electro-optic bottlenecks, network nodes can become quite complex since they have to perform the switching operations.

Network architectures with very low hardware requirements and significantly simplified network management can be realized by moving the switching functions toward the network periphery [3]-[7]. The core of the resulting passive network is an arrayed-waveguide grating (AWG). This wavelength sensitive device makes spatial wavelength reuse possible. In [8], this kind of concurrency is termed *network division*; due to the wavelength selectivity of an AWG each source can reach only small parts of the network by choosing the corresponding wavelength. On other parts of the network additional transmissions can take place simultaneously as opposed to broadcast-and-select WDM networks which are based on a passive star coupler (PSC). Each terminal contains a tunable transmitter/receiver pair. The resulting single-hop network has no switches and buffers at all. Single-hop WDM networks are superior to their multihop counterparts with regard to average hop distance and channel utilization since no system capacity is lost due to data forwarding. Moreover, processing requirements at each node are reduced since stations have to process only packets which are addressed to them. Reduced nodal protocol processing requirements are an important issue in very high-speed networks. However, in single-hop WDM networks transmitters and/or receivers have to be tunable. Most reported single-hop WDM networks are based on the PSC [9]. In this paper, we investigate PSC and AWG based single-hop WDM networks and compare them in terms of throughput, delay and blocking probability. In addition, upper bounds for traffic shaping are provided. We do not present a novel medium access protocol. Instead, we analyze both architectures by using a simple round-robin time division multiplexing (TDM) scheme. The analysis presented in the appendix does not take into account queueing delay but still provides valuable insight into the performance of both architectures.

The remainder of the paper is organized as follows. In Section II, we briefly outline the properties of the PSC and the AWG. In Section III, we discuss the merits and limitations of spatial wavelength reuse. Section IV explains the network architectures and the channel assignment. Numerical results are presented in Section V. Section VI concludes

This work was supported in part by Deutsche Telekom AG. This paper was presented in part at the Optical Network Workshop, UT Dallas, TX, January 31 - February 1, 2000

The authors are with the Telecommunication Networks Group, Technical University of Berlin, D-10587 Berlin, Germany (e-mail: maier@ee.tu-berlin.de).

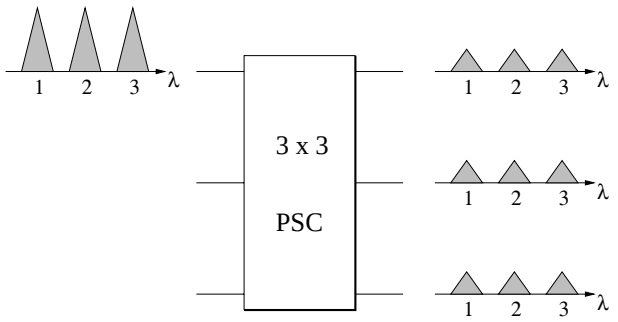

Fig. 1. Broadcasting and splitting loss of a 3×3 passive star coupler (PSC)

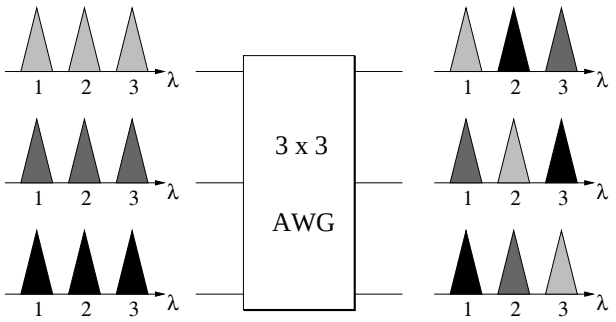

Fig. 2. Wavelength routing and spatial wavelength reuse of a 3×3 arrayed-waveguide grating (AWG)

the paper.

II. Properties of PSC and AWG

The PSC is a passive multiport broadcast-and-select device. It is not a wavelength sensitive WDM component. Wavelengths launched onto any input port are broadcast to every output port. This is illustrated in Fig. 1 for three wavelengths coming into the upper input port of a 3×3 PSC. Ignoring the excess loss, the optical input power is equally distributed to the output ports. Each output port receives only a portion of the original power. In case of an $N \times N$ star coupler the resulting splitting loss equals $10 \log_{10} N$ (dB).

The PSC can be implemented as an integrated optics planar device in which the star coupler and the waveguides are fabricated on a semiconductor, glass (silica) or polymer substrate [10]. Alternatively, an $N \times N$ PSC can be made out of $\frac{N}{2} \log_2 N$ 2×2 couplers (assuming N is a power of 2) [11].

PSC based WDM networks offer a better power budget than optical bus networks. This is due to the fact that WDM bus networks suffer from tapping loss which linearly depends on the number of attached nodes. In contrast, the splitting loss in WDM star networks, as mentioned above, grows only logarithmically with the number of nodes. Therefore, the PSC is the preferred device to realize broadcast-and-select single-hop WDM networks such as Bellcore's LAMBDANET [12], IBM's RAINBOW [13], or STARNET at Stanford University [14]. In addition, the PSC can also be used to build switches [15] and much research was done in the area of medium access control (MAC) protocols for PSC based single-hop networks such as [16][17][18].

Broadcasting is reasonable for signaling purposes such as pretransmission coordination in single-hop networks where transmitters and/or receivers are tunable. In this case generally, a transmitter sends a control packet on a common control channel to inform the intended destination about time and wavelength of the corresponding data packet transmission. Since the control packet is broadcast, all other nodes receive the control packet as well – provided all nodes listen to the control channel. Thus, all nodes have global knowledge and can use it to avoid collisions resulting in an improved network throughput-delay performance. For data transmission, however, broadcasting wastes precious bandwidth and optical power since data packets are sent to all nodes even though most packets are destined only to a single or a few nodes. Consequently, the PSC is not suitable for networks without signaling such as WDM networks with fixed channel assignment. PSC based broadcast-and-select networks do not provide privacy and do not allow spatial wavelength reuse.

The AWG is a passive wavelength routing device. It is a polarization independent and wavelength selective WDM component [19][20]. In contrast to the PSC, spatial wavelength reuse is possible with AWGs. This is shown in Fig. 2 for a 3×3 AWG where three wavelengths are fed into all AWG input ports. To schematically illustrate the wavelength routing characteristics of the AWG, wavelengths launched onto the same input port are shaded identically. As can be seen, every wavelength can be used on all input ports simultaneously without channel collision since the AWG is a wavelength routing device. (Note that successfully transmitted packets can still experience receiver collisions, i.e., the intended receiver is tuned to another wavelength. This problem has to be addressed by appropriate access protocols.) To date, the AWG has mainly been used to realize WDM components such as add-drop multiplexer (ADM) [21], discretely tunable filter and equalizer [22][23], optical cross-connect (OXC) [24], multifrequency laser (MFL) [25], packet synchronizer [26] or simple multiplexer/demultiplexer, which can be deployed for example in passive optical networks (PONs) [27].

The AWG and wavelength routing devices in general unicast packets and consequently do not suffer from splitting loss resulting in an improved power budget. Data packets destined to a single station do not take more bandwidth than necessary enabling spatial wavelength reuse. Since there is no broadcasting the AWG is predestined for WDM networks which do not require pretransmission coordination via a common broadcast control channel. (Note that broadcasting could be realized by spectrally slicing a broadband LED signal. But this approach is not further considered in the present work.)

III. Spectrum Reuse

In the previous section we have seen that unlike the PSC the AWG allows spatial wavelength reuse, i.e., each wavelength can be applied at all AWG input ports simultaneously. Ideally, each wavelength is routed to a different output port without channel collision and crosstalk. However, real devices suffer from leakage [28]. As a consequence, each wavelength is routed not only to the intended AWG output port but is received in part at the remaining output ports as well. The resulting crosstalk has the same wavelength as the proper signal and cannot be removed by a demultiplexer at the destination which in turn puts limitations on network scalability [29]. This intrachannel crosstalk causes signal-crosstalk homodyne beat noise and has a detrimental impact on the bit error rate (BER). The resulting power penalty is given by

$$P = -5 \log_{10} \left[1 - 4q^2 N 10^{\epsilon_{dB}/10} \right] \quad (1)$$

where ϵ_{dB} is the component crosstalk in dB and $q = 5.9$ for a BER of 10^{-9} [30]. Note that the power penalty does not depend on the bit rate. Fig. 3 depicts the worst case power penalty for matched polarization of the crosstalk signals versus the component crosstalk for $N \in \{1, 2, 4, 8, 16, 32, 100\}$, where N denotes the wavelength reuse factor.

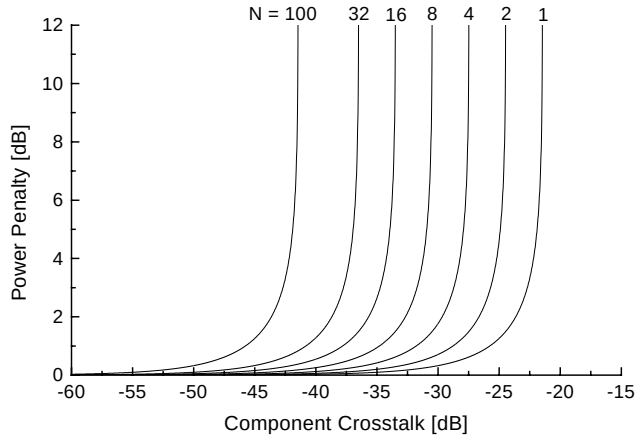

Fig. 3. Power penalty vs. component crosstalk

Thus, wavelength reuse in WDM networks is possible only with a certain power penalty. For example, an AWG with a component crosstalk of -35 dB can sustain an eight times reuse of each wavelength with a power penalty of 1 dB. An AWG with a component crosstalk of -39 dB was reported in [31]. Such a low crosstalk increases spatial wavelength reuse. Even much higher spectrum reuse factors with a negligible power penalty can be achieved if the AWG is realized not as a planar but free-space device which provides a component crosstalk of less than -60 dB [32].

Spatial wavelength reuse provides a higher degree of concurrency. Thus, more transmissions can take place simultaneously. Given N input ports, a PSC can support up to N transmissions at the same time whereas up to N^2 simultaneous transmissions are possible using an AWG. Note that in this paper only one single free spectral range (FSR) of the AWG is exploited, i.e., in case of an $N \times N$ AWG N wavelengths are used. The FSR is the period of the wavelength response of a wavelength selective optical device. As a consequence, for N simultaneously transmitting stations in AWG based single-hop networks the wavelength pool can be kept small and only $\lceil \sqrt{N} \rceil$ wavelengths are required (where $\lceil x \rceil$ denotes the smallest integer which is larger than or equal to x) whereas in PSC based single-hop networks the number of wavelengths grows linearly with the number of simultaneously transmitting nodes, i.e., N wavelengths are required. The relation between the number of simultaneously transmitting nodes and the number of required wavelengths for PSC and AWG based single-hop WDM networks is depicted in Fig. 4. As shown, especially for a larger population, the AWG needs significantly fewer wavelengths than the PSC. Hence, AWG based single-hop networks can use transceivers with a limited tuning range even for a larger population. For example, for 256 simultaneously transmitting nodes a 16×16 AWG with a channel spacing of 0.8 nm requires transceivers with a tuning range of 12 nm as opposed to 204 nm in case of a PSC. Table I shows that the AWG can apply electro-optic transceivers

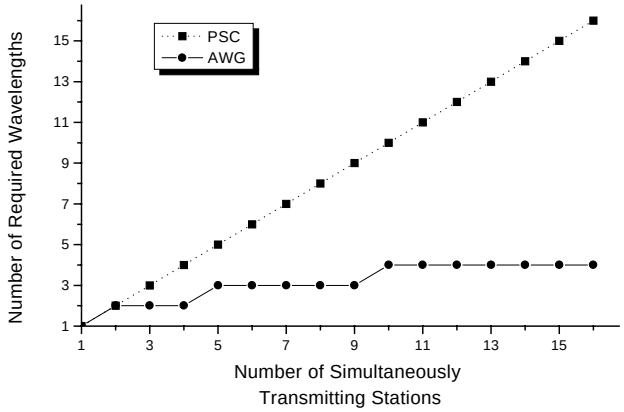

Fig. 4. Relation between wavelength pool size and population

	Electro-optic transceiver	Acousto-optic transceiver	Mechanically tunable transceiver
Tuning range	$10 - 15$ nm	~ 100 nm	500 nm
Tuning time	$1 - 10$ ns	~ 10 μs	$1 - 10$ ms

TABLE I

Tuning ranges and tuning times for different transceiver types

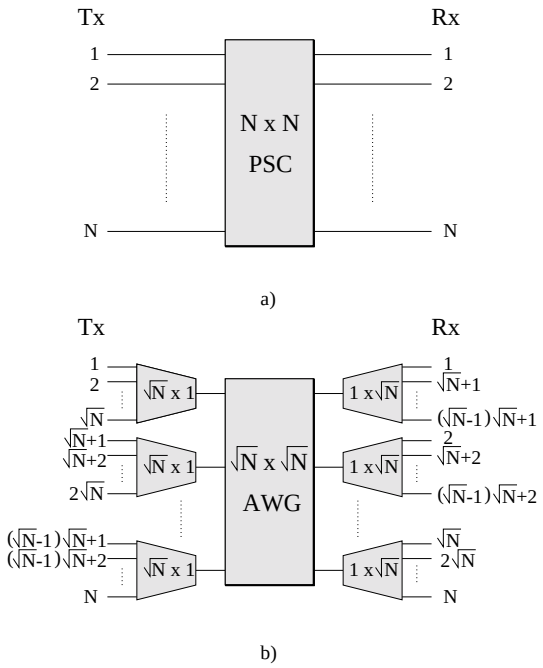

Fig. 5. Single-hop network architecture: a) PSC based, b) AWG based

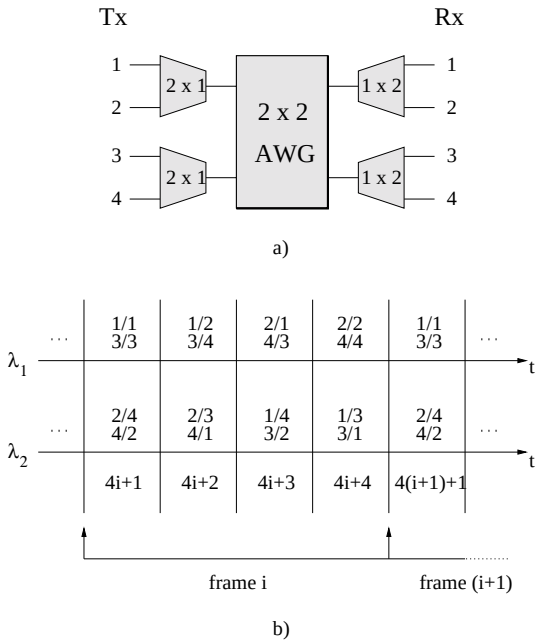

Fig. 6. a) AWG based architecture without cyclic receiver attachment, b) fixed channel assignment (N=4)

whose tuning time is six orders of magnitude smaller than that of mechanically tunable transceivers which would be necessary for the PSC. Moreover, the PSC can support fewer stations due to the fact that the maximum tuning range of mechanically tunable transceivers is approached earlier. Since transceiver tuning times have a strong impact on the network performance large gain in efficiency can be achieved by using transceivers whose tuning time is as small as possible. Owing to wavelength reuse, nodes in AWG based single-hop WDM networks can still apply fast tunable transceivers while nodes in PSC based networks already have to utilize acoustooptic or even mechanically tunable transceivers whose tuning times are three or six orders of magnitude larger, respectively. Due to the significantly smaller transceiver tuning latency, AWG based single-hop WDM networks are expected to outperform their PSC counterparts in terms of throughput and delay.

IV. Architecture

We compare a PSC and an AWG based single-hop network architecture. Both networks connect N stations (Fig. 5). Each of the N stations has one transmitter and one receiver, which are tunable over the entire range of N (PSC) and $\sqrt{N}$ (AWG) wavelengths, respectively (for the sake of simplicity $\sqrt{N}$ is assumed to be an integer; otherwise, $\left\lceil \sqrt{N} \right\rceil$ wavelengths are required). In case of the AWG, both transmitter and receiver have to be tunable to enable full interconnection. A $\sqrt{N} \times 1$ combiner is attached to each input port of the $\sqrt{N} \times \sqrt{N}$ AWG. Every combiner collects the signals of $\sqrt{N}$ transmitters each of them sending on a different wavelength at any time to avoid channel collisions. Similarly, each AWG output signal is distributed via a $1 \times \sqrt{N}$ splitter to $\sqrt{N}$ receivers (splitting factor $1/\sqrt{N}$). On each AWG port $\sqrt{N}$ transmissions can take place simultaneously. In total, there are N stations transmitting over $\sqrt{N}$ wavelengths simultaneously as opposed to N wavelengths in the PSC based network. The splitting loss introduced by the splitters has a less severe impact on the power budget if the single-hop architecture is based on an AWG. With a PSC instead of an AWG the splitting factor is $1/N$ instead of $1/\sqrt{N}$, i.e., the splitting loss is twice as big (in dB).

Note that in the AWG based network the receivers are attached in a cyclic manner. The reason for the cyclic receiver attachment is illustrated for $N = 4$. Fig. 6 a) depicts the architecture without cyclic receiver attachment. Since we have seen that the AWG is predestined for single-hop WDM networks which do not require pretransmission coordination via a common broadcast control we apply a fixed time division multiplexing (TDM) round-robin channel assignment scheme which is shown schematically in Fig. 6 b) where X/Y denotes transmitter X and receiver Y. Apparently, bandwidth is wasted by slots where $X = Y$. All these slots are assigned only to wavelength λ_1. If the transceivers are attached in a cyclic manner to the splitters as shown in Fig. 7 a), the channel assignment is changed as depicted in Fig. 7 b). The first slot of each frame can be omitted since it contains only transmitter-receiver pairs where the transmitter and the receiver belong to the same station. Thus, bandwidth is saved by reducing the frame length. This idea is valid for arbitrary N. In general, receiver i is attached to splitter j according to the following rule

$$j \quad = \quad \left[(i-1) \ mod \ \sqrt{N} \right] + 1$$

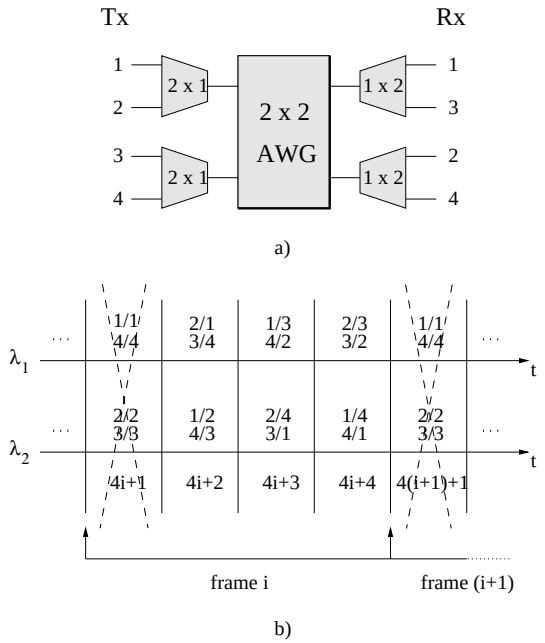

Fig. 7. a) AWG based architecture with cyclic receiver attachment, b) fixed channel assignment with reduced frame length (N=4)

$$, \quad i \in \{1,2,\ldots,N\}, j \in \{1,2,\ldots,\sqrt{N}\}. \quad (2)$$

The resulting frame contains $N-1$ slots providing full connectivity. Both channel and receiver collisions are eliminated. The round-robin TDM access scheme is chosen for comparative performance evaluation of both architectures. Such a fixed channel assignment is mainly attractive for uniform nonbursty traffic and at medium to high system loads. For bursty traffic, however, a MAC protocol which dynamically allocates bandwidth to the nodes is expected to provide better performance.

As mentioned above, a fixed round-robin TDM channel assignment scheme is used. All channels are slotted with a slot length equal to the packet transmission time plus the transceiver tuning time. The length of the packets is assumed to be constant. Transceivers are switched on a per packet basis. The tuning overhead results in a decreased channel utilization and in a significantly reduced network capacity C which is equal to the total number of transmitted packets per packet transmission time and is given by

$$C = \frac{N \cdot Utilization}{E[H]} = \frac{N}{1+\tau} \quad (3)$$

where time is normalized to the packet transmission time, N denotes the number of simultaneously transmitting stations, $E[H]$ denotes the mean hop distance which is unity in single-hop networks and τ is the normalized transceiver tuning time. Fig. 8 depicts the network capacity (maximum network throughput) for a 32×32 AWG and a PSC. The channel spacing is assumed to be 100 GHz (0.8 nm at 1.55 μm). Packets have a constant length of 10^4 bits. All channels are slotted. A slot is composed of the packet transmission time and the transceiver tuning time. The required tuning range grows with increasing

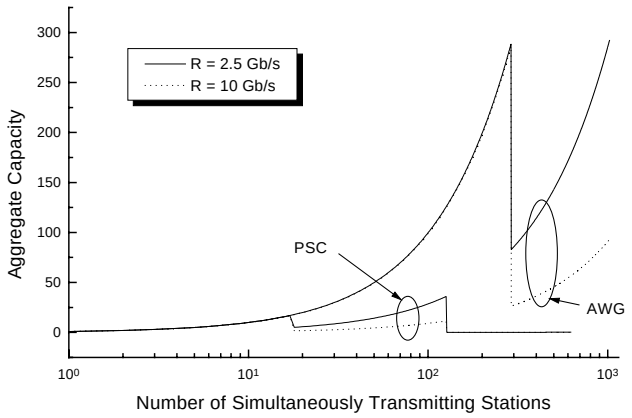

Fig. 8. Aggregate capacity (packets/packet transmission time) vs. number of simultaneously transmitting stations (R denotes the transmission rate)

number of stations. Obviously, the AWG provides a significantly higher aggregate capacity and a larger maximum number of simultaneous transmissions. The edges represent the transitions from electro-optical to acoustooptical transceivers and from acoustooptical to mechanically tunable transceivers, respectively. With each transition the tuning latency is increased which in turn reduces the capacity. As shown, the PSC reaches these transitions earlier than the AWG. Due to wavelength reuse the AWG can deploy fast tunable transceivers up to about 300 stations and is able to sustain the maximum of $32^2 = 1024$ station by using acoustooptical transceivers. In contrast, the PSC cannot support more than 626 simultaneous transmissions due to the limited tuning range of optical transceivers. For lower transmission rates the packet transmission time and thereby the channel utilization are increased resulting in an improved aggregate capacity.

V. Numerical Results

In this section AWG and PSC are compared in terms of throughput, delay and packet loss for different values of N. The analysis is presented in the appendix. The analysis assumes that each station is equipped with N *single-packet* buffers, one for reception and $N-1$ for transmission. The arrival process to each single-packet buffer is assumed to be Poisson with a mean arrival rate λ. In both cases, N stations simultaneously transmit in a fixed round-robin fashion. While the AWG requires only $\sqrt{N}$ wavelengths (recall that $\lceil\sqrt{N}\rceil$ wavelengths are used if $\sqrt{N}$ is not an integer) the PSC requires exactly N wavelengths. The channel spacing is assumed to be 200 GHz (1.6 nm at 1.55 μm). Fast tunable transceivers are assumed to have a tuning range of 10 nm and a tuning time of 10 ns while acoustooptic transceivers are assumed to be tunable over a range of 100 nm with a tuning time of 10 μs. As a result, fast tunable transceivers can be applied as long as the number of wavelengths is not larger than 7. Packets are

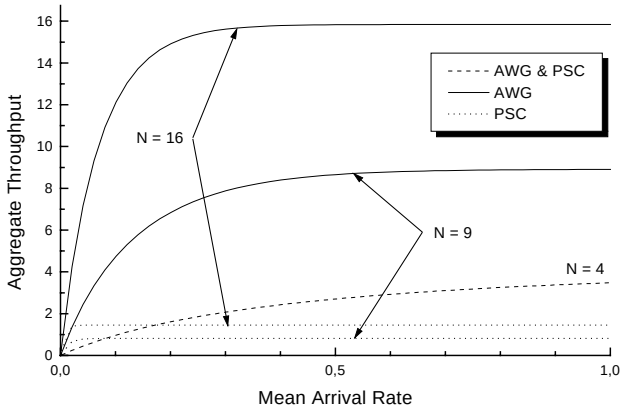

Fig. 9. Aggregate throughput (packets/packet transmission time) vs. average arrival rate (packet/packet transmission time)

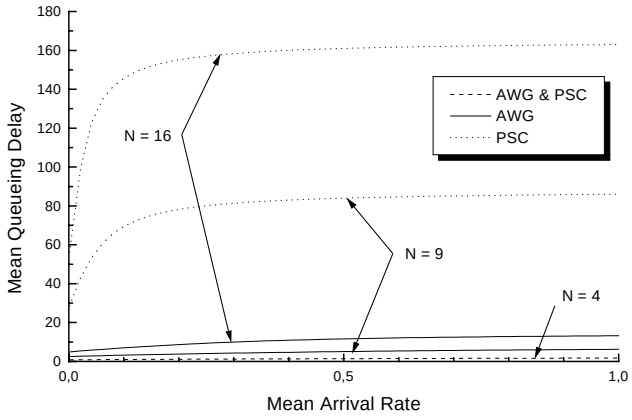

Fig. 10. Mean queueing delay (packet transmission time) vs. average arrival rate (packet/packet transmission time)

assumed to contain 10^4 bits and the channel transmission rate equals 10 Gb/s. Thus, the normalized tuning time τ equals 10^{-2} for electro-optic transceivers and 10 for acoustooptic transceivers. Recall that each slot is composed of the packet transmission time and the transceiver tuning time. For illustration we show plots for small values of $N \in \{4, 9, 16\}$. As we will see, for increasing N the performance difference between AWG and PSC becomes even more dramatic.

The throughput (packets/packet transmission time) vs. the average arrival rate (packet/packet transmission time) is shown in Fig. 9. As shown, the AWG clearly outperforms the PSC. For $N = 4$ the wavelength pool is small enough to use fast tunable transceivers for both AWG and PSC. Whereas, for $N \in \{9, 16\}$ electro-optic transceivers can be deployed only for the AWG. For the PSC, acoustooptic transceivers whose tuning time is three orders of magnitude larger have to be used. Consequently, the channel utilization decreases significantly resulting in a reduced aggregate throughput. In general, the aggregate throughput grows with increasing mean arrival rate. Apparently, the PSC curves run into saturation earlier (i.e., at lower loads); because of the longer slot and thereby frame duration a user is more likely backlogged when the corresponding slot is assigned to it. In case of the AWG the maximum aggregate throughput is almost N due to the negligible tuning time of electro-optic transceivers. For higher values of N the throughput increases for both AWG and PSC since more channels lead to higher concurrency resulting in an improved system throughput and saturation is reached earlier. This is due to the fact that for both AWG and PSC the frame length is proportional to N. Therefore, for larger N (longer frame) a user is more likely backlogged when a slot is assigned to it. For larger N the throughput difference between AWG and PSC becomes more evident.

In Fig. 10 the mean queueing delay (packet transmission time) vs. the average arrival rate (packet/packet transmission time) for nonblocked packets is shown. Again,

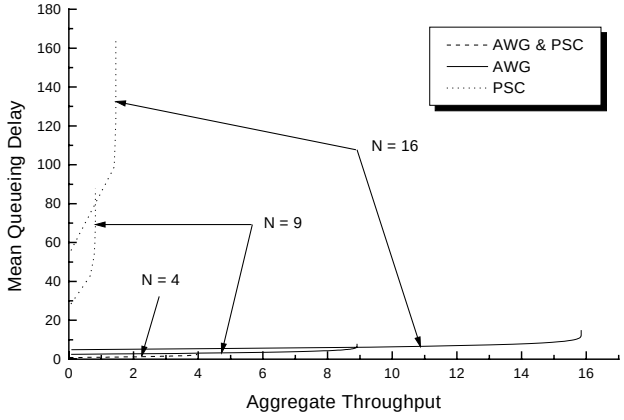

Fig. 11. Mean queueing delay (packet transmission time) vs. aggregate throughput (packets/packet transmission time)

the AWG exhibits a significantly better delay characteristic than the PSC, especially for larger N. In both cases, the mean queueing delay increases for higher values of N. This is due to the longer frame length. Note again that for larger N the difference between AWG and PSC becomes more dramatic and both systems run into saturation earlier. For infinite arrival rates both AWG and PSC approach asymptotically the maximum value which is identical to the frame length which is $(N-1)(1+\tau)$. Again, for $N \in \{9, 16\}$ fast tunable transceivers can be deployed only for the AWG. Hence, for these values of N the delay characteristics of the AWG are much better. The mean queueing delay is limited since the applied analytical model is based on a single-packet buffer per user. Hence, if the buffer already contains one packet new arriving packets are discarded and do not contribute to the mean queueing delay.

Fig. 11 illustrates the mean queueing delay (packet transmission time) vs. aggregate throughput (packets/packet

transmission time) for nonblocked packets. This figure points out that for large N the AWG clearly outperform the PSC from the view point of throughput and delay.

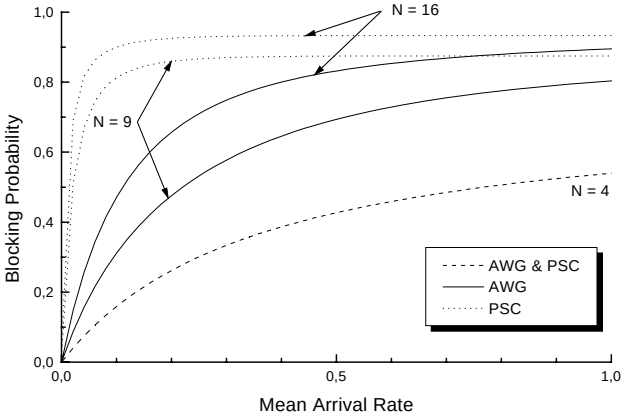

Fig. 12. Blocking probability vs. mean arrival rate (packet/packet transmission time)

The blocking probability vs. the mean arrival rate (packet/packet transmission time) is depicted in Fig. 12. Compared to the AWG, for a given mean arrival rate and $N \in \{9, 16\}$ backlogged stations have to wait longer in case of the PSC and new arriving packets are more likely to find the buffer already full. All curves asymptotically approach unity since all buffers are occupied continuously for an infinite arrival rate. This state is reached earlier, i.e., at lower loads, for large N due to the longer frame length. Obviously, already for small N the blocking probability is quite high. Such high loss rates are not acceptable. However, in real systems each station has large buffers. Thus, arriving packets are put in the queue and are not blocked resulting in a significantly reduced blocking probability. Even though the analysis does not consider queueing for the sake of simplicity, the results provide a valuable insight into the performance of both systems.

Larger buffers are not needed and yet high aggregate throughput at a very low blocking probability can be achieved by traffic shaping, i.e., the random arrivals have to be made deterministic. Note that such traffic shaping is relatively easy for networks with fixed channel assignment since the delay is bounded. This upper limit is used by the traffic shaper to control the packet arrival rate and to avoid buffer overflow, i.e., packet loss. Fig. 13 shows the upper bound of the traffic shaper transmission rate which is given by

$$Rate \leq \frac{1}{(N-1)(1+\tau)}, \tag{4}$$

where again N denotes the number of simultaneously transmitting stations and τ is the normalized transceiver tuning time. For larger transmission rates we have an increased normalized tuning time τ resulting in a decreased upper transmission rate bound. No packets are lost if the traffic shaper transmits packets at a rate less or equal to this upper bound, i.e., no more than one packet per user and per cycle is transmitted by the traffic shaper. The queueing delay in the single-packet buffer is bounded and cannot be larger than the number of slots between two successive transmission permissions (cycle length) which is given by

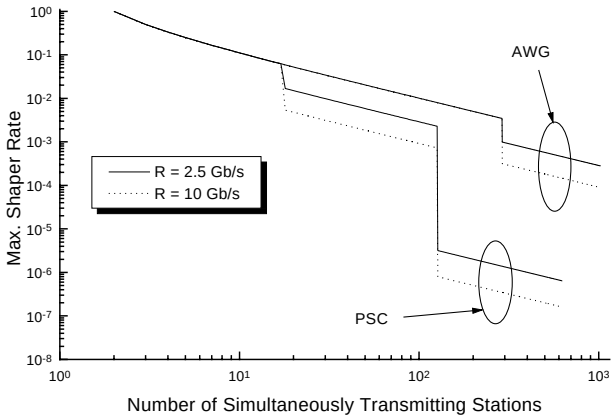

Fig. 13. Maximum shaper transmission rate (packet/packet transmission time) vs. number of simultaneously transmitting stations (R denotes the transmission rate)

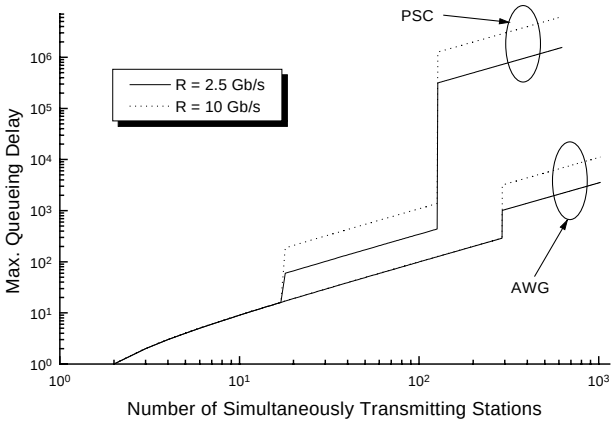

Fig. 14. Maximum queueing delay (packet transmission time) vs. number of simultaneously transmitting stations (R denotes the transmission rate)

$$Queueing\ delay \leq (N-1)(1+\tau) \tag{5}$$

and is illustrated in Fig. 14. Again, a higher transmission rate implies an increased τ which in turn increases the upper queueuing delay bound.

VI. Conclusion and Future Work

In this paper we have compared PSC and AWG based single-hop WDM networks. Single-hop networks provide a number of advantages such as high channel utilization

and low nodal processing requirements. Moreover, the network management is dramatically simplified by distributing the switching operation toward the network periphery. Such single-hop WDM networks are well suited for realizing metro networks. Since the AWG is a wavelength-routing device each wavelength can be spatially reused. Due to the low crosstalk of an AWG the power penalty is relatively low. Wavelength reuse keeps the number of required wavelengths small. This in turn enables the deployment of transceivers with a significantly smaller tuning time. It was shown that for a fixed round-robin channel assignment AWG based single-hop WDM networks are superior to their PSC based counterparts in terms of throughput and mean queueing delay. Yet, the high packet loss rates are not acceptable in practical systems. One possibility for decreasing this loss rate is the usage of buffers such as optical delay lines. However, this causes an increased delay. Another possibility is to apply a sophisticated medium access control (MAC) protocol. We expect that a properly chosen dynamic MAC protocol could substantially reduce the loss rate.

Future work will focus on AWG based networks with dynamic channel allocation using an adequate MAC protocol. For signaling we have to find a way to realize broadcasting. This is not trivial since AWGs do not inherently support broadcasting. In addition, issues such as multicasting and variably sized packets will be addressed. Multicasting is quite useful to improve the network throughput-delay performance due to the increased receiver throughput.

VII. Acknowledgement

The authors would like to thank Dr. Martin Reisslein for his helpful comments.

Appendix

For the throughput-delay performance analysis the source/destination allocation protocol analytic approach reported in [33] was slightly modified in order to accomodate wavelength reuse and packet loss.

There are N stations simultaneously transmitting over $\sqrt{N}$ wavelengths in case of the AWG and over N wavelengths in case of the PSC. Each station can transmit/receive one packet at a time on/from any of the channels. Every station has N single-packet buffers, one for reception and $N-1$ for transmission. Thus, the interconnections between each pair of nodes can be modeled independently. Each buffer represents an independent (virtual) user (i,j), $1 \leq i,j \leq N$. The packet length is assumed to be constant. Time is normalized to the packet transmission time. Time is divided into cycles which contain $N-1$ slots. Each slot is composed of the packet transmission time (unity) and the normalized transceiver tuning time τ. Every pair of virtual users is assigned one slot per cycle. The arrival process is assumed to be Poisson with the average arrival rate of λ packets per time unit per user. An idle user is defined as a user with an empty buffer and a backlogged user is defined as a user with a packet for transmission. Arriving packets are discarded if the user is backlogged, i.e., the buffer is full. The traffic between any pair of users is assumed to have the same mean arrival rate λ.

The allocation matrix $U(t)$ is a $N \times N$ matrix whose elements $u_{ij}(t)$ represent the channel number on which user (i,j) can transmit in slot t, $t = 1,2,\ldots,N-1$ and $1 \leq i,j \leq N$. $W(t)$ is a binary matrix with the elements $w_{ij}(t) = Ind(u_{ij}(t) > 0)$, where the indicator function is given by

$$Ind(statement) = \begin{cases} 1 & \text{, if } statement \text{ true} \\ 0 & \text{, if } statement \text{ false .} \end{cases} \tag{6}$$

The allocation matrix $U(t)$ is subject to the following conditions:

- $\sum_i w_{ij}(t) \leq 1$, i.e., no receiver collisions occur
- $\sum_i \sum_j w_{ij}(t) = N$, i.e., the number of simultaneous transmissions is restricted to N
- In case of the PSC, for every $w_{ij}(t) \neq 0$: $u_{ij}(t) \neq u_{kl}(t)$ if $i \neq k$ and $j \neq l$, i.e., no channel collisions occur
- In case of the AWG, for every $w_{ij}(t) \neq 0$: $u_{ij}(t) \neq u_{kl}(t)$ if $\left\lceil \frac{i}{\sqrt{N}} \right\rceil = \left\lceil \frac{k}{\sqrt{N}} \right\rceil$ and $i \neq k, j \neq l$, i.e., no channel collisions occur
- $\sum_j w_{ij}(t) \leq 1$, i.e., a station can transmit on at most one channel

The system is observed at the regeneration points embedded at the beginning of each slot. The throughput of user (i,j), defined as the number of successfully transmitted packets of user (i,j) per slot is given by

$$S_{ij} = \frac{1}{(N-1)(1+\tau)} \sum_{t=1}^{N-1} w_{ij}(t) \cdot \pi_{ij}(t), \tag{7}$$

where $\pi_{ij}(t)$ denotes the steady-state probability that user (i,j) is backlogged (packet in buffer) at the beginning of slot t. Hence, the system throughput, defined as the total number of successfully transmitted packets per slot can be obtained by

$$S = \sum_{\forall i} \sum_{\forall j} S_{ij}. \tag{8}$$

To evaluate the aggregate throughput $\pi_{ij}(t)$ is needed. The probability $\pi_{ij}(t)$ can be expressed as a function of the probability $\pi_{ij}(t-1)$, mean packet arrival rate and the matrix $W(t)$:

$$\begin{aligned} \pi_{ij}(t) &= [1-\pi_{ij}(t-1)]\left(1-e^{-\lambda(1+\tau)}\right) \\ &\quad + \pi_{ij}(t-1)\left[1-w_{ij}(t-1)\right] \\ &= \pi_{ij}(t-1)\left[e^{-\lambda(1+\tau)} - w_{ij}(t-1)\right] \\ &\quad + \left(1+e^{-\lambda(1+\tau)}\right) \quad , 2 \leq t \leq N-1. \end{aligned} \tag{9}$$

This leads to the following recursive formula

$$\begin{aligned} \pi_{ij}(t) &= \pi_{ij}(1) \prod_{k=1}^{t-1} \left[e^{-\lambda(1+\tau)} - w_{ij}(k)\right] + \\ &\quad + \left(1-e^{-\lambda(1+\tau)}\right). \end{aligned}$$

$$\cdot \left\{ \sum_{l=2}^{t-1} \prod_{k=l}^{t-1} \left[e^{-\lambda(1+\tau)} - w_{ij}(k) \right] + 1 \right\}$$
$$, \; 2 \leq t \leq N-1. \qquad (10)$$

Assuming the system is in steady state, we equate

$$\pi_{ij}(N) = \pi_{ij}(1). \qquad (11)$$

Substituting (11) in (10), we obtain

$$\pi_{ij}(1) = \left(1 - e^{-\lambda(1+\tau)}\right) \cdot \frac{\sum_{l=2}^{N-1} \prod_{k=l}^{N-1} \left[e^{-\lambda(1+\tau)} - w_{ij}(k) \right] + 1}{1 - \prod_{k=1}^{N-1} \left[e^{-\lambda(1+\tau)} - w_{ij}(k) \right]} \qquad (12)$$

and for $2 \leq t \leq N-1$ we finally obtain

$$\pi_{ij}(t) = \left(1 - e^{-\lambda(1+\tau)}\right) \cdot \frac{\sum_{l=2}^{N-1} \prod_{k=l}^{N-1} \left[e^{-\lambda(1+\tau)} - w_{ij}(k) \right] + 1}{1 - \prod_{k=1}^{N-1} \left[e^{-\lambda(1+\tau)} - w_{ij}(k) \right]} \cdot \prod_{k=1}^{t-1} \left[e^{-\lambda(1+\tau)} - w_{ij}(k) \right] + \left(1 - e^{-\lambda(1+\tau)}\right) \cdot \left\{ \sum_{l=2}^{t-1} \prod_{k=l}^{t-1} \left[e^{-\lambda(1+\tau)} - w_{ij}(k) \right] + 1 \right\}. \qquad (13)$$

Using Little's Law, the mean packet delay of user (i,j), defined as the average time between the arrival of a packet at user (i,j) and the beginning of its transmission is given by

$$D_{ij} = \frac{Q_{ij}}{S_{ij}} \qquad (14)$$

where Q_{ij} denotes the mean backlog (over time) at user (i,j). For the average packet delay in the system we obtain

$$D = \sum_{\forall i} \sum_{\forall j} \frac{S_{ij}}{S} D_{ij}. \qquad (15)$$

For the evaluation of Q_{ij} we introduce the following definitions

- r_{ij}: the number of transmission permissions per cycle (note that in the considered channel allocation scheme $r_{ij} = 1, 1 \leq i,j \leq N$)
- *idle period*$_{ij}$: the time interval between two consecutive grantings of permissions to user (i,j), or between a permission and the cycle boundary
- n_{ij}: the number of *idle period*$_{ij}$ intervals of user (i,j) in the allocation cycle
- s_{ijl}: the number of idle slots in the l-th *idle period*$_{ij}$ $(1 \leq l \leq n_{ij})$

First, we calculate $Res(s_{ijl}, \lambda)$ which denotes the expected value of the residual time user (i,j) is backlogged in the l-th *idle period* with the length of s_{ijl} slots.

$$Res(s_{ijl}, \lambda) = \int_0^{s_{ijl}(1+\tau)} [s_{ijl}(1+\tau) - t] \lambda e^{-\lambda t} dt = \frac{e^{-\lambda s_{ijl}(1+\tau)} + \lambda s_{ijl}(1+\tau) - 1}{\lambda}. \qquad (16)$$

Q_{ij} is obtained by the weighted average of the residual time in each idle period

$$Q_{ij} = \sum_{k=1}^{n_{ij}} \frac{s_{ijk}}{(N-1) - r_{ij}} \cdot \frac{Res(s_{ijk}, \lambda)}{s_{ijk} \cdot (1+\tau)} = \sum_{k=1}^{n_{ij}} \frac{e^{-\lambda(1+\tau) \cdot s_{ijk}} + \lambda(1+\tau) \cdot s_{ijk} - 1}{[(N-1) - r_{ij}] \cdot \lambda(1+\tau)}. \qquad (17)$$

Thus, using equations (8) and (15) the network throughput and the average queueing delay can be evaluated.

The blocking probability is equal to the probability that an arriving packet finds the station backlogged. Assuming uniform traffic all virtual users behave identically. Thus, any arbitrary virtual user, say (i,j), can be considered. Using (12) and (13) the blocking probability P_B can be obtained by

$$P_B = \frac{1}{N-1} \sum_{t=1}^{N-1} \pi_{ij}(t). \qquad (18)$$

References

[1] B. Mukherjee, "WDM-Based Local Lightwave Networks - Part II: Multihop Systems", *IEEE Network Mag.*, vol. 6, no. 4, pp. 20-32, July 1992

[2] S. Yao and B. Mukherjee, "Advances in Photonic Packet Switching: An Overview", *IEEE Commun. Mag.*, vol. 38, no. 2, pp. 84-94, Feb. 2000

[3] N. P. Caponio, A. M. Hill, F. Neri, R. Sabella, "Single-Layer Optical Platform Based on WDM/TDM Multiple Access for Large-Scale "Switchless" Networks", *European Trans. on Telecommun.*, vol. 11, no. 1, pp. 73-82, Jan./Feb. 2000

[4] A. Bianco, E. Leonardi, M. Mellia, F. Neri, "Network Controller Design for SONATA, a Large Scale All-Optical WDM Network", *Proc., Optical Network Workshop 2000*, UT Dallas, TX, Jan./Feb. 2000

[5] S. Binetti, G. Notaro, and R. Sabella, "Transmission Features and Limitations of Large-Scale Switchless All-Optical Networks", *IEEE Photon. Technol. Lett.*, vol. 11, no. 7, pp. 913-915, July 1999

[6] A. Yu, M. J. O'Mahony and A. M. Hill, "Transmission limitation of all-optical network based on $N \times N$ multi/demultiplexer", *Elect. Lett.*, vol. 33, no. 12, pp. 1068-1069, June 1997

[7] A. M. Hill, M. Brierley, R. M. Percival, R. Wyatt, *et al.*, "Multiple-Star Wavelength-Router Network and Its Protection Strategy", *IEEE J. Select. Areas in Commun.*, vol. 16, no. 7, pp. 1134-1145, Sept. 1998

[8] T. Matsumoto and H. Ishio, "Multiple-Access Optical Network Architecture Employing a Wavelength-and-Network-Division Technique: MANDALA", *IEICE Trans. on Commun.*, vol. E82-B, no. 9, pp. 1439-1445, Sept. 1999

[9] B. Mukherjee, "WDM-Based Local Lightwave Networks - Part I: Single-Hop Systems", *IEEE Network Mag.*, vol. 6, no. 3, pp. 12-27, May 1992

[10] B. Mukherjee, "Optical Communication Networks", *McGraw-Hill*, 1997

[11] R. Ramaswami, K. N. Sivarajan, "Optical Networks - A Practical Perspective", *Morgan Kaufmann*, 1998

[12] M. S. Goodman, H. Kobrinski, M. P. Vecchi, R. M. Bulley, J. L. Gimlett, "The LAMBDANET Multiwavelength Network: Architecture, Applications, and Demonstrations", *IEEE J. Select. Areas in Commun.*, vol. 8, no. 6, pp. 995-1004, Aug. 1990

[13] E. Hall, J. Kravitz, R. Ramaswami, M. Halvorson, *et al.*, "The Rainbow-II Gigabit Optical Network", *IEEE J. Select. Areas in Commun.*, vol. 14, no. 5, pp. 814-823, June 1996

[14] L. G. Kazovsky, P. T. Poggiolini, "STARNET: A Multi-gigabit-per-second Optical LAN Utilizing a Passive WDM Star", *IEEE/OSA J. Lightwave Technol.*, vol. 11, no. 5/6, pp. 1009-1027, May/June 1993

[15] E. Arthurs, M. S. Goodman, H. Kobrinski, M. P. Vecchi, "HYPASS: An Optoelectronic Hybrid Packet Switching System",

IEEE J. Select. Areas in Commun., vol. 6, no. 9, pp. 1500-1510, Dec. 1988

[16] F. Jia, B. Mukherjee, "The Receiver Collision Avoidance (RCA) Protocol For A Single-Hop WDM Lightwave Network", *IEEE/OSA J. Lightwave Technol.*, vol. 11, no. 5/6, pp. 1053-1065, May/June 1993

[17] I. Chlamtac, and A. Fumagalli, "Quadro-Star: A High Performance Optical WDM Star Network", *IEEE Trans. on Commun.*, vol. 42, no. 8, pp. 2582-2591, Aug. 1994

[18] A. Ganz, Y. Gao, "Time-Wavelength Assignment Algorithms for High Performance WDM Star Based Systems", *IEEE Trans. on Commun.*, vol. 42, no. 2/3/4, pp. 1827-1836, Feb./March/April 1994

[19] H. Takahashi, K. Oda, H. Toba, and Y. Inoue, "Transmission Characteristics of Arrayed Waveguide $N \times N$ Wavelength Multiplexer", *IEEE/OSA J. Lightwave Technol.*, vol. 13, no. 3, pp. 447-455, March 1995

[20] N. J. Frigo, I. P. Kaminow, T. L. Koch, *Optical Fiber Telecommunications*, vol. IIIA, pp. 461-522, 1997

[21] Y. Tachikawa, Y. Inoue, M. Kawachi, H. Takahashi and K. Inoue, "Arrayed-waveguide grating add-drop multiplexer with loop-back optical paths", *Elect. Lett.*, vol. 29, no. 24, pp. 2133-2134, Nov. 1993

[22] Y. Tachikawa, Y. Inoue, M. Ishii, and T. Nozawa, "Arrayed-Waveguide Grating Multiplexer with Loop-Back Optical Paths and Its Applications", *IEEE/OSA J. Lightwave Technol.*, vol. 14, no. 6, pp. 977-984, June 1996

[23] B. Glance, I. P. Kaminow, and R. W. Wilson, "Applications of the Integrated Waveguide Grating Router", *IEEE/OSA J. Lightwave Technol.*, vol. 12, no. 6, pp. 957-962, June 1994

[24] K. A. McGreer, "Arrayed Waveguide Gratings for Wavelength Routing", *IEEE Commun. Mag.*, pp. 62-68, Dec. 1998

[25] M. Zirngibl, "Multifrequency Lasers and Applications in WDM Networks", *IEEE Commun. Mag.*, pp. 39-41, Dec. 1998

[26] A. Franzen, D. K. Hunter, I. Andonovic, "A Low Loss Optical Packet Synchronisation Architecture", *Proc., SPIE*, vol. 3531, Boston, MA, pp. 390-395, Nov. 1998

[27] M. Zirngibl, C. H. Joyner, L. W. Stulz, C. Dragone, *et al.*, "LARNet, a Local Access Router Network", *IEEE Photon. Tech. Lett.*, vol. 7, no. 2, pp. 215-217, Feb. 1995

[28] H. Takahashi, K. Oda, and H. Toba, "Impact of Crosstalk in an Arrayed-Waveguide Multiplexer on $N \times N$ Optical Interconnection", *IEEE/OSA J. Lightwave Technol.*, vol. 14, no. 6, pp. 1097-1105, June 1996

[29] L. Gillner, C. P. Larsen, and M. Gustavsson, "Scalability of Optical Multiwavelength Switching Networks: Crosstalk Analysis", *IEEE/OSA J. Lightwave Technol.*, vol. 17, no. 1, pp. 58-67, Jan. 1999

[30] E. L. Goldstein, and L. Eskildsen, "Scaling Limitations in Transparent Optical Networks Due to Low-Level Crosstalk", *IEEE Photon. Technol. Lett.*, vol. 7, no. 1, pp. 93-94, Jan. 1995

[31] K. Takada, H. Yamada and Y. Inoue, "Origin of channel crosstalk in 100 GHz spaced silica-based arrayed-waveguide grating multiplexer", *Elect. Lett.*, vol. 31, no. 14, pp. 1176-1177, July 1995

[32] A. M. Hill, S. Carter, J. Armitage, M. Shabeer, *et al.*, "A Scalable and Switchless Optical Network Structure, Employing a Single 32×32 Free-Space Grating Multiplexer", *IEEE Photon. Technol. Lett.*, vol. 8, no. 4, pp. 569-571, April 1996

[33] I. Chlamtac, A. Ganz, "Channel Allocation Protocols in Frequency-Time Controlled High Speed Networks", *IEEE Trans. on Commun.*, vol. 36, no. 4, pp. 430-440, April 1988